BIOCHEMISTRY
including biophysical chemistry & molecular biology

Article

pubs.acs.org/biochemistry

Trinucleotide Repeat DNA Alters Structure To Minimize the Thermodynamic Impact of 8-Oxo-7,8-dihydroguanine

Catherine B. Volle,[†] Daniel A. Jarem,[§] and Sarah Delaney*[,§]

[†]Department of Molecular and Cellular Biology and Biochemistry and [§]Department of Chemistry, Brown University, Providence, Rhode Island 02912, United States

Supporting Information

ABSTRACT: In the phenomenon of trinucleotide repeat (TNR) expansion, an important interplay exists between DNA damage repair of 8-oxo-7,8-dihydroguanine (8-oxoG) and noncanonical structure formation. We show that TNR DNA adapts its structure to accommodate 8-oxoG. Using chemical probe analysis, we find that CAG repeats composing the stem−loop arm of a three-way junction alter the population of structures in response to 8-oxoG by positioning the lesion at or near the loop. Furthermore, we find that oligonucleotides composed of odd-numbered repeat sequences, which form populations of two structures, will also alter their structure to place 8-oxoG in the loop. However, sequences with an even number of repeats do not display this behavior. Analysis by differential scanning calorimetry indicates that when the lesion is located within the loop, there are no significant changes to the thermodynamic parameters as compared to the DNA lacking 8-oxoG. This contrasts with the enthalpic destabilization observed when 8-oxoG is base-paired to C and indicates that positioning 8-oxoG in the loop avoids the thermodynamic penalty associated with 8-oxoG base-pairing. Since formation of stem−loop hairpins is proposed to facilitate TNR expansion, these results highlight the importance of defining the structural consequences of DNA damage.

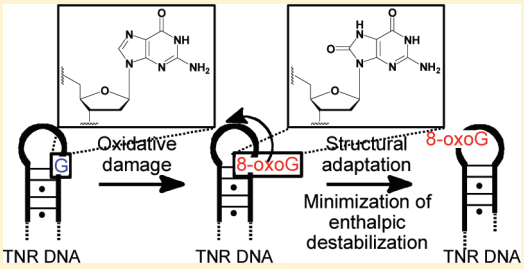

Cellular DNA is constantly bombarded with reactive oxygen species (ROS) from both intra- and extracellular sources.[1] Of the four DNA nucleobases, guanine (G) has the lowest redox potential[2] and is most readily oxidized by ROS. A commonly observed form of oxidatively damaged DNA is 8-oxo-7,8-dihydroguanine (8-oxoG).[3] Interestingly, 8-oxoG is able to rotate about the glycosidic bond to convert from the canonical *anti* conformation to the *syn* conformation. When in the *syn* conformation, 8-oxoG can base pair with A via Hoogsteen bonding. Because of its ability to pair with A, 8-oxoG is mutagenic and can cause G to T transversion mutations if this mispair is not repaired prior to replication. In order to maintain genetic integrity, 8-oxoG is removed from DNA by the repair protein 8-oxo-7, 8-dihydroguanine glycosylase (Ogg1), which recognizes the modified G and catalyzes cleavage of the *N*-glycosidic linkage to the sugar−phosphate backbone.[4]

Surprisingly, while repair of DNA damage is usually beneficial, removal of 8-oxoG by Ogg1 has been implicated in the expansion of CAG/CTG trinucleotide repeat (TNR) sequences.[5−7] CAG/CTG repeats in exon 1 of the huntingtin gene are genetically unstable and their expansion provides the molecular basis for Huntington's disease (HD).[8] Using a mouse model of HD, expansion at CAG/CTG repeat tracts was abrogated in mice lacking Ogg1.[5] Subsequent work *in vitro* led to the proposal of a "toxic oxidation cycle" fueling the expansion of CAG/CTG repeats.[5,6] As part of this cycle, Ogg1 removes 8-oxoG from duplex DNA and polymerase β performs strand-displacement synthesis, incorporating multiple nucleotides as part of a long-patch base excision repair (LP-BER) event. The formation of a noncanonical structure by the displaced flap, a TNR stem−loop hairpin, renders the DNA refractory to cleavage by flap endonuclease, and ligase incorporates the stem−loop hairpin into the DNA, causing expansion. Additionally, we have shown that the stem−loop hairpin formed by the displaced flap is hypersusceptible to oxidation and that Ogg1 does not efficiently remove 8-oxoG from the stem−loop hairpin.[9,10] We proposed that this combination of susceptibility to oxidation and inefficient repair would exacerbate TNR expansion during LP-BER.[10]

While we have previously shown that a TNR stem−loop hairpin is more susceptible than duplex to oxidative damage, the effect of this damage on the structure and stability of the DNA has not been defined. Substrates that are expanded during LP-BER are differentiated from substrates that are properly repaired by the formation of noncanonical structures. Thus, given the known propensity for damage to accumulate in the noncanonical structure formed by TNR sequences, it is necessary to define the structural and thermodynamic impact of this damage. Here we provide a structural analysis of TNR DNA containing 8-oxoG. We find that TNR DNA has the ability to modulate its structure to accommodate 8-oxoG, both in the context of a three-way junction and in single-stranded oligonucleotides. Furthermore, we show that this structural

Received: October 7, 2011
Revised: November 17, 2011
Published: December 7, 2011

change minimizes the thermodynamic impact of the DNA lesion. The implications of these findings on TNR expansion are discussed.

EXPERIMENTAL PROCEDURES

Oligonucleotide Synthesis and Purification. Oligonucleotides were synthesized using standard phosphoramidite chemistry on a BioAutomation DNA/RNA synthesizer. The oligonucleotides containing 8-oxoG were synthesized trityl-off (on instrument removal of the 5′-dimethoxytrityl group), and the oligonucleotides were deprotected in 1 M β-mercaptoethanol in NH_4OH at 55 °C for 24 h. Two rounds of HPLC purification were then carried out using a Dionex DNAPac PA100 anion-exchange column (4 × 250 mm) using 10% acetonitrile (solvent A) and 0.8 M ammonium chloride in 10% acetonitrile (solvent B) as the mobile phases (gradient: solvent B was increased from 55% to 75% over 5 min, then 75% to 90% over 15 min, and 90% to 100% over 5 min; 1 mL/min).

For the synthesis of oligonucleotides lacking 8-oxoG, the 5′-trityl group was retained to facilitate purification by HPLC. Purification of these oligonucleotides was performed on a Dynamax Microsorb C18 column (10 × 250 mm) using acetonitrile (solvent A) and 30 mM ammonium acetate (solvent B) as the mobile phases (gradient: solvent A was increased from 5% to 25% over 25 min; 3.5 mL/min). Following removal of the 5′-trityl group by incubation in 80% glacial acetic acid for 12 min at room temperature, the oligonucleotides were subjected to a second round of HPLC purification (gradient: solvent A was increased from 0% to 15% over 35 min; 3.5 mL/min). The longer sequences used to construct the three-way junctions were purified as described above, but an additional gel purification step was performed after HPLC to ensure removal of longer failure sequences. Samples were suspended in denaturing loading buffer (80% formamide, 10 mM EDTA, 1% xylene cyanol), applied to a 14% denaturing polyacrylamide gel, and electrophoresed at 80 W until the dye had migrated 8 in. The DNA was then excised and eluted from the gel by crushing and soaking. The supernatant, containing the purified DNA, was collected and desalted using Sephadex G50 fine resin.

Chemical Probe Analysis. Oligonucleotides were 5′-^{32}P end-labeled using T4 polynucleotide kinase (New England Biolabs) following the manufacturer's protocol. 10 pmol of labeled DNA was suspended in 100 μL of Tris buffer (20 mM Tris-HCl, 70 mM NaCl, 10 mM EDTA, pH 7.5), heated to 90 °C for 5 min, and slowly cooled to room temperature. Samples were then divided to 2 pmol per aliquot, mixed with 5 μg of calf thymus DNA, and brought to 100 μL total volume before being incubated with either 1% DEPC (v/v) or 0.05% DMS in ethanol (v/v) for 5−30 min at 37 °C. Reactions were quenched by addition of 20 μL of stop solution (1.5 M sodium acetate, 1 M β-mercaptoethanol, 250 μg/mL tRNA, pH 7.0), ethanol precipitated, and the pellet dried *in vacuo*. Samples were then treated with 10% piperidine (v/v) for 30 min at 90 °C before drying *in vacuo*. Samples were resuspended in denaturing loading buffer (80% formamide, 10 mM EDTA, 1% xylene cyanol, 1% bromophenol blue), incubated at 90 °C for 3 min before loading onto a 16% denaturing polyacrylamide gel. Samples were electrophoresed at 80 W until the xylene cyanol and bromophenol blue dyes were separated by 4 in. The products were visualized by phosphorimagery, using a BioRad FX scanner and the accompanying Quantity One software. Histograms were generated by drawing a line through the lane corresponding to the 15 min time point and were background subtracted using the "rolling ball" technique with the radius set to 25.

Three-way junction constructs were formed by annealing 10 pmol of radiolabeled CAG16-TWJ or CAG16-8-TWJ with a 1.5-fold excess of the complementary sequence CTG6-TWJ. DEPC reactions on the three-way junction constructs were performed using 2.5% DEPC (v/v) and incubated for 5−30 min at 37 °C. Sample work-up was the same as above except that samples were run on a 14% gel.

Differential Scanning Calorimetry. Calorimetry was performed using a TA Instruments NanoDSC III. Oligonucleotides were suspended in 700 μL of 20 mM sodium phosphate, 70 mM NaCl, pH 7.5. All samples were degassed *in vacuo* for 12 min at 25 °C before analysis. Data were obtained by monitoring the excess power required to maintain the same temperature in both the sample cell and a reference cell filled with degassed buffer. Each cycle of the experiment consists of a forward scan, in which the temperature is raised from 10 to 95 °C at a rate of 1 °C/min, a reverse scan, in which the temperature is decreased from 95 to 10 °C at 1 °C/min, and an equilibration period of 10 min between each forward and reverse scan. The resulting thermograms display the excess heat capacity (C_p) as a function of temperature. Ten thermograms, consisting of both forward and reverse scans, were obtained for each DNA substrate. The thermograms were normalized for concentration, background corrected using a buffer−buffer scan, and a polynomial baseline correction was performed using the NanoAnalyze software after fitting the linear portions of the pre- and post-transitional baseline. ΔH was determined by integrating the area under the excess heat capacity curve. ΔS was determined by plotting C_p/T against the temperature in K and integrating under the resulting curve. ΔG was calculated at 37 °C using the values obtained for ΔH and ΔS and the equation $\Delta G = \Delta H - T\Delta S$ where T is in K.

RESULTS AND DISCUSSION

Structural Characterization of a TNR Three-Way Junction. A DNA three-way junction mimics a genomic repeat tract after an expansion has occurred, where there are more CAG repeats present than complementary CTG repeats. To determine the influence of 8-oxoG on these postexpansion TNR sequences, we used a chemical probe of nucleobase solvent accessibility to investigate the structure of three-way junctions by revealing the presence of loops, bulges, or overhangs. These three-way junctions contain 16 CAG repeats, six of which base pair with a CTG repeat in the complementary strand, and the remaining ten are predicted to form a stem−loop hairpin. We have shown previously that a single strand containing 10 CAG repeats adopts a stem−loop hairpin in which the loop contains four nucleobases and G-C base pairs and A·A mismatches comprise the stem.[9,11,12] Here, the stem−loop hairpin is flanked by duplex in order to form a three-way junction. Furthermore, the CAG/CTG repeats are bordered by a well-matched duplex comprised of a mixed sequence.

The first three-way junction lacks 8-oxoG and was assembled using the sequences CAG16-TWJ and CTG6-TWJ (Table 1); this three-way junction, which lacks damage, serves as a control. In the second three-way junction, G8 in CAG16-TWJ is site-specifically replaced by 8-oxoG, where G8 refers to the guanine in the eighth CAG repeat when counting from the 5′-end of the TNR sequence (CAG16-TWJ-8OX). Because of the repetitive nature of the sequence in these three-way junctions, it is

dx.doi.org/10.1021/bi201552s | *Biochemistry* 2012, 51, 52−62

Table 1. DNA Sequences Used in This Study

name	nucleotide sequence[a]
CAG16-TWJ	5′-(CCTTAGCTCC)$(CAG)_{16}$(TAAGGGGAAC)-3′
CAG16-8OX-TWJ	5′-CCTTAGCTCC)$(CAG)_7$(CAG^{ox})$(CAG)_8$(TAAGGGGAAC)-3′
CTG6-TWJ	5′-(GTTCCCCTTA)$(CTG)_6$(GGAGCTAAGG)-3′
CAG7	5′-$(CAG)_7$-3′
CAG10	5′-$(CAG)_{10}$-3′
CAG11	5′-$(CAG)_{11}$-3′
CAG15	5′-$(CAG)_{15}$-3′
CAG7-3′Overhang	5′-$(CAG)_2$(CTTTTG)$(CAG)_3$-3′
CAG7-5′Overhang	5′-$(CAG)_3$(CTTTTG)$(CAG)_2$-3′
CAG7-Blunt Stem	5′-$(CAG)_2$(CTTTTTTTG)$(CAG)_2$-3′
CAG10-5OX	5′-$(CAG)_4(CAG^{ox})(CAG)_5$-3′
CAG10-6OX	5′-$(CAG)_5(CAG^{ox})(CAG)_4$-3′
CAG11-5OX	5′-$(CAG)_4(CAG^{ox})(CAG)_6$-3′
CAG11-6OX	5′-$(CAG)_5(CAG^{ox})(CAG)_5$-3′

[a] G^{ox} represents 8-oxo-7,8-dihydroguanine.

expected that the CAG stem−loop can position itself in several ways relative to the six complementary CTG repeats. Indeed, such behavior was confirmed by structural analysis using the chemical probe diethyl pyrocarbonate (DEPC), a small molecule that reveals the solvent accessibility of purines, with preferential modification of adenines.[13] Upon incubation with DEPC, the CAG16-TWJ/CTG6-TWJ substrate shows hyperreactivity at A6 through A12 (Figure 1A, Supporting Information Figure S1A), though interestingly, we do not observe equal reactivity at these adenines. This result indicates that the CAG stem−loop hairpin forms at six of the seven possible positions along the complement but that each of these structures does not form in equal amounts. Based on the level of reactivity at A11 and A12, which exhibit the highest degree of modification by DEPC, the top structure in Figure 1A is most likely predominant within the population. The composition of the flanking duplex regions may skew the formation of stem−loop hairpins. Indeed, while we had anticipated that the stem−loop would be able to occupy all seven positions, the two G−C base pairs flanking the first CAG repeat may limit the dynamics of the system and prevent the first CAG repeat from being part of the stem.

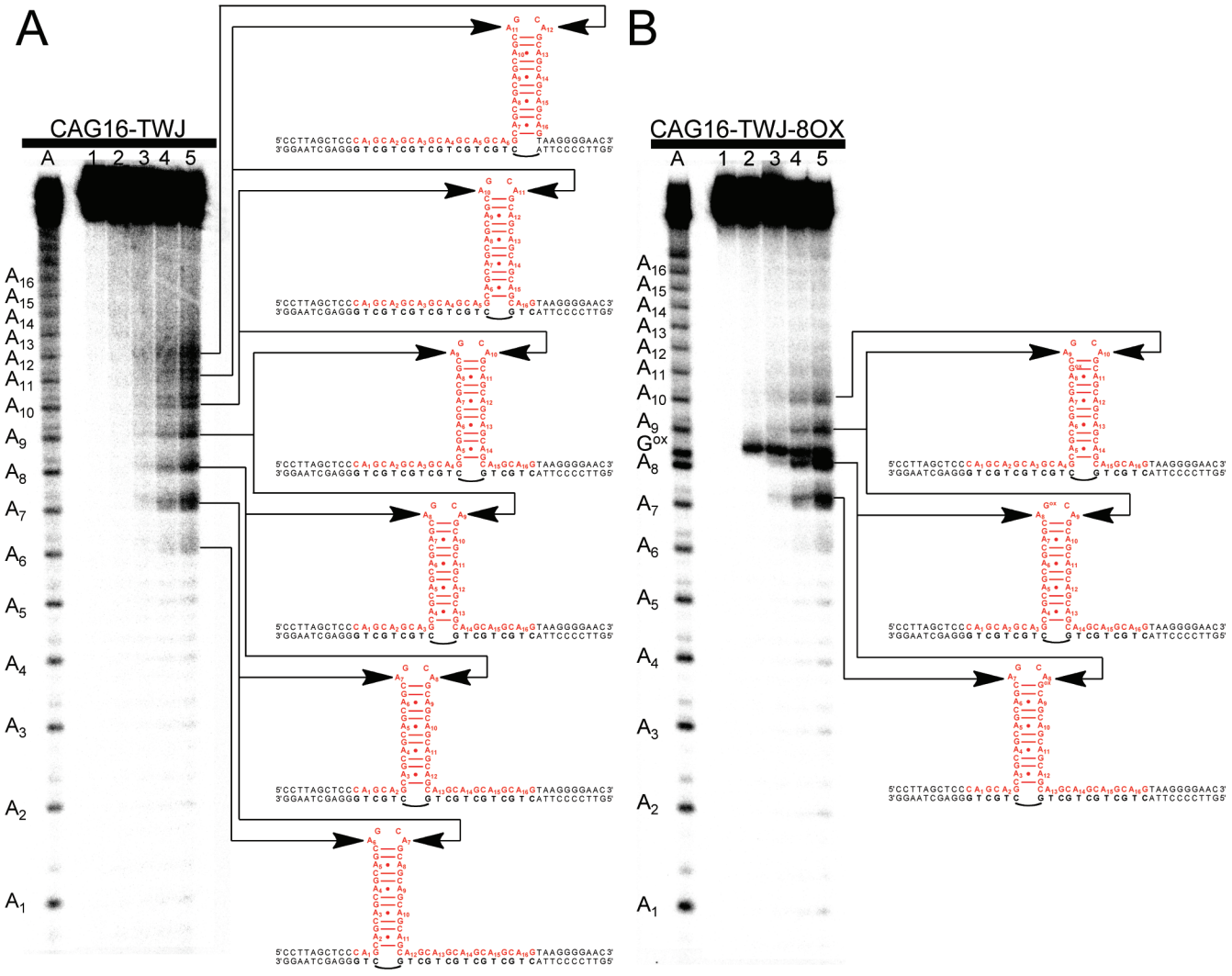

Figure 1. Autoradiogram of DEPC reactions with (A) CAG16-TWJ/CTG6-TWJ and (B) CAG16-TWJ-8OX/CTG6-TWJ. Lanes 1 are DNA alone, lanes 2 are piperidine-treated DNA, and lanes 3−5 are DNA treated with 2.5% (v/v) DEPC at 37 °C for 5, 15, or 30 min, respectively, followed by treatment with piperidine. Lanes A are a marker created by treatment of the single-stranded CAG16-TWJ or CAG16-TWJ-8OX substrate with 1% DEPC at 37 °C for 15 min. The proposed structures derived from the reactivity of each substrate are shown to the right of the autoradiogram.

dx.doi.org/10.1021/bi201552s | *Biochemistry* 2012, 51, 52−62

Notably, on the basis of reactivity toward DEPC, we propose that the CAG repeats form a stem−loop hairpin as part of the three-way junction and not an open bulge in which there is no intrastrand hydrogen bonding between the CAG repeats. In a bulge, every adenine in the CAG repeat region would be unpaired and solvent accessible and thus highly reactive toward DEPC. Furthermore, since a bulge would be able to shift its position relative to the CTG repeats in the complementary sequence, A2 through A16 would be equally accessible and modifiable by DEPC. Because of the lack of intense, ubiquitous DEPC reactivity at these adenines, we conclude that the CAG repeats in the three-way junction form a stem−loop hairpin and not a bulge. In fact, the formation of a stem−loop limits the solvent accessibility of the adenines in the stem and protects these nucleobases from modification by DEPC.

Recent work using the fluorescent adenine analogue 2-aminopurine (2-AP), which exhibits increased florescence with increasing solvent exposure, has shown that a stem−loop hairpin, and not an open bulge, is formed by 15 CAG repeats when part of a three-way junction.[14] Interestingly, 8 CAG repeats adopt an open bulge, not a structured stem−loop, in the context of a three-way junction, but form a structured stem−loop when the TNR sequence is not part of a three-way junction.[15,16] Degtyareva and co-workers proposed that in the shorter tract of 8 CAG repeats folding into a stem−loop is disrupted by A·A mismatches in the stem and by base-pairing in the flanking duplex regions.[16] Indeed, we propose here that the flanking duplex regions influence the likelihood of formation of the CAG stem−loop at various positions along the complementary CTG repeats.

In order to determine the extent to which 8-oxoG alters the structure of the three-way junction, we replaced a G in the CAG stem−loop with 8-oxoG. Importantly, when 8-oxoG is introduced into the eighth repeat, in the center of the CAG repeats, the observed hyper-reactivity to DEPC is restricted to adenines A7 through A10 (Figure 1B and Figure S1B). Strand cleavage is also observed at the 8-oxoG (Supporting Information Discussion). This pattern of reactivity corresponds to the formation of the stem−loop at three of the seven potential positions along the CTG complement. These results can be compared to those obtained in the absence of 8-oxoG, in which A6 through A12 were hyper-reactive to DEPC and the CAG stem−loop formed at six of the seven potential positions along the CTG complement. Importantly, the loss of hyper-reactivity at certain adenines indicates that 8-oxoG is modulating the location where the stem−loop forms within the repeat tract.

When considering the amount of reactivity to DEPC at each adenine in CAG16-TWJ-8OX/CTG6-TWJ, these structures seem to position the 8-oxoG directly either in the loop or in the base pairs nearest the loop, eliminating the structures where the lesion is positioned further down the stem (Figure 1B). We hypothesize that positioning the lesion at or near the loop within the three-way junction could decrease or eliminate the enthalpic penalty associated with 8-oxoG-C base-pairing, as it is known that 8-oxoG base-paired with C in a duplex confers an enthalpic destabilization to the structure.[17−19] To better understand the behavior of the three-way junction, it is advantageous to study the behavior of the stem−loop component alone; this approach will allow us to better address the combination of structural and energetic influences 8-oxoG has on TNR DNA.

Influence of 8-OxoG on the Structure of an Even-Numbered TNR Sequence. Since we observed that the structure of the CAG16-TWJ-8OX/CTG6-TWJ sequence is modulated in order to position 8-oxoG in or near the loop, we wondered if 8-oxoG would have a similar effect on the TNR sequence when removed from the three-way junction. To investigate the inherent ability of 8-oxoG to impact the structure of TNR DNA outside the context of a three-way junction, we performed chemical probe experiments with CAG10 (Table 1), as this mimics the stem−loop of the three-way junction.

When incubated with DEPC, the CAG10 substrate shows reactivity at every A, with increased reactivity at A5 and A6, indicating their presence in a loop (Figure 2A). A histogram displaying a graphical representation of the reactivity of CAG10 is provided in Figure 2B. Furthermore, when incubated with the chemical probe dimethyl sulfate (DMS), which reveals the solvent accessibility of guanines,[20] reactivity is observed at every G with hyper-reactivity at G5 (Figure S2A,B), consistent with G5 being positioned in a loop. This pattern of reactivity to DEPC and DMS indicates the formation of a four nucleobase loop that includes A5, G5, C6, and A6 and a blunt-ended stem (Figure 2B). Interestingly, the two reactive adenines in the loop, A5 and A6, are not modified to the same extent by DEPC. This difference in reactivity may derive from differences in stacking interactions with the adjacent nucleobases, as we proposed in earlier work.[11] The folding of CAG10 into a stem−loop is consistent with the structures observed for several other TNRs, including those comprised of CAG, CTG, CGG, and CCG repeats, which have been shown to form stem−loop hairpins *in vitro*.[9−12,14−16,21−30]

It is important to note that while hyper-reactivity to chemical probes was observed at particular adenines and guanines, some level of reactivity was observed at every A and G in CAG10. Indeed, this result is consistent with the established reactivity patterns of DEPC and DMS. DEPC is known to modify unpaired adenines in loops, bulges, and overhangs, but not adenines in well-matched A−T base pairs.[31,32] However, the adenines in the stem of the TNR hairpins are part of A·A mismatches, which are known to have increased dynamics relative to an A−T base pair,[33] and therefore we would expect these adenines to be modified by DEPC, although to a lesser extent than the unpaired adenines in the loop region. DMS is known to modify guanines in G−C base pairs,[20] and we observed modification of such guanines in the stem region; however, unpaired guanines, such as those in the loop, are modified to a greater extent due to increased accessibility to DMS. Interestingly, we observe only slight modification by DEPC of the adenines in the stem of the three-way junctions, and only for the longest incubation time; the flanking duplex regions may minimize the dynamics of the stem, leading to less modification by DEPC.

In order to determine the extent to which 8-oxoG influences the structure of CAG10, we site-specifically replaced G5 or G6 with 8-oxoG to form CAG10-5OX and CAG10-6OX, respectively. When an 8-oxoG is present in the CAG10 TNR sequence, the reactivity to DEPC and DMS indicates that the overall stem−loop structure does not change and that the position of the four nucleobase loop and the presence of a blunt-ended stem are maintained (Figure 2C,D, Figure S2C,D, and Supporting Information Discussion). However, while the overall stem−loop structure is maintained, there are subtle differences in the DEPC reactivity profile when 8-oxoG is

dx.doi.org/10.1021/bi201552s | *Biochemistry* 2012, 51, 52−62

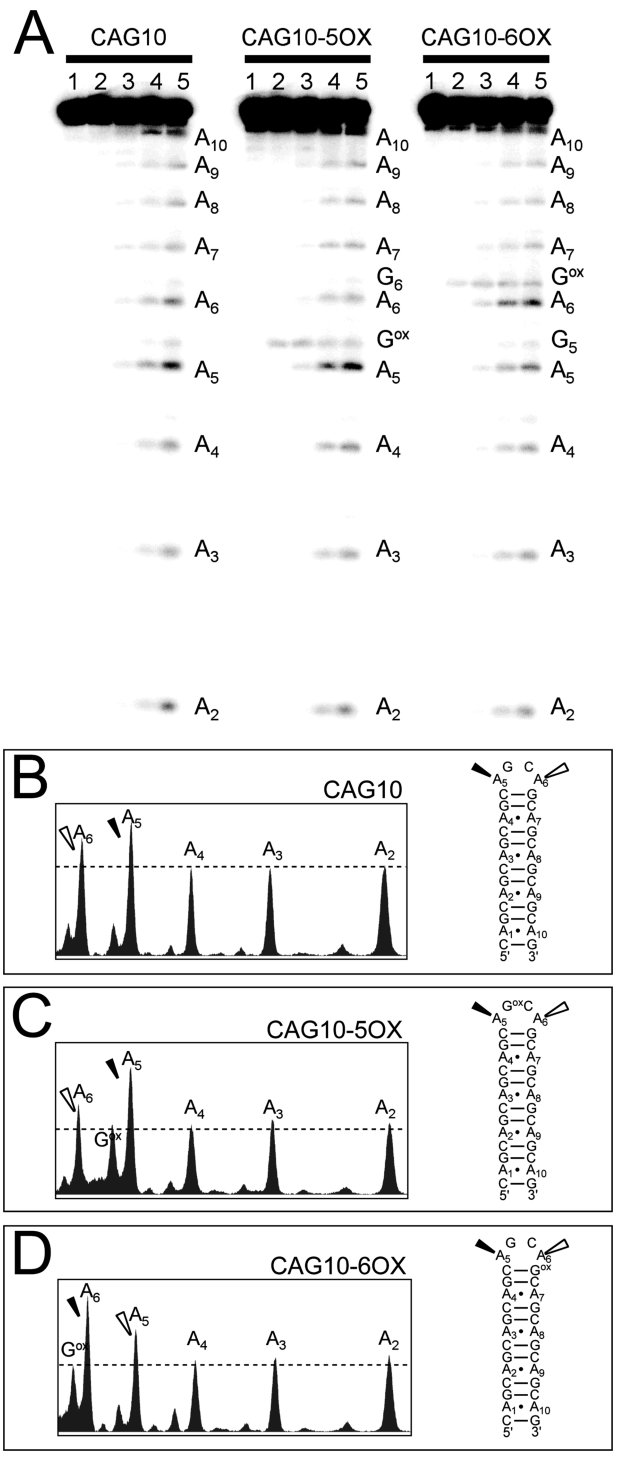

Figure 2. (A) Autoradiogram of DEPC reactions with CAG10, CAG10-5OX, and CAG10-6OX. Lanes 1 are DNA alone, lanes 2 are piperidine-treated DNA, and lanes 3−5 are DNA treated with 1% (v/v) DEPC at 37 °C for 5, 15, or 30 min, respectively, followed by treatment with piperidine. Histograms of DEPC reactivity, derived from lanes 4, with (B) CAG10, (C) CAG10-5OX, and (D) CAG10-6OX. The dashed line in each histogram demarks the level of reactivity of adenines in the stem region, which serves as a baseline to establish hyper-reactivity of the nucleobases in the loop. Proposed structures for CAG10, CAG10-5OX, and CAG10-6OX are shown next to the corresponding histogram. The closed wedge indicates hyper-reactivity to DEPC and the open wedge indicates moderate hyper-reactivity to DEPC.

present; notably, we observe an increase in the reactivity of the adenine 5′ to the 8-oxoG. In fact, of all the adenines in CAG10-5OX, A5 exhibits the highest reactivity to DEPC (Figure 2C), while A6 of the CAG10-6OX substrate exhibits the highest reactivity to DEPC (Figure 2D). The observation of differing levels of solvent accessibility near an 8-oxoG is consistent with the recent work of Singh and co-workers, which demonstrated that 8-oxoG has a disruptive effect on a base pair 5′ of an 8-oxoG-C base pair.[19] Our data indicate that 8-oxoG can exert a similar effect within a single-stranded DNA loop.

To confirm the presence of a blunt-ended stem in CAG10-5OX and CAG10-6OX, we performed DMS reactions to monitor the reactivity of G1 and G2. In particular, if the 8-oxoG in CAG10-6OX were to be repositioned into the loop, a two repeat overhang would form at the 5′ end, leading to greater reactivity to DMS of the guanines in those repeats. We observed no increase in DMS reactivity at G1 or G2, consistent with a blunt-ended stem (Figure S2C,D). Thus, all three CAG10 substrates, regardless of the presence of 8-oxoG, form hairpins with a four nucleobase loop and a blunt-ended stem (Figure 2B−D). Therefore, unlike the effects exhibited by 8-oxoG in the three-way junction, the presence of 8-oxoG in CAG10 results only in minor changes to the solution accessibility of the adjacent nucleobase and does not dramatically alter the overall structure adopted by the sequence.

Recent work from our laboratory has indicated that single strands containing an odd number of CTG repeats, the complement of CAG, form populations composed of two structures, both with four nucleobase loops and either a 3′ or a 5′ overhang.[12] We hypothesized that if odd-numbered CAG repeats exhibit the same behavior, they may have the ability to reposition and better accommodate the lesion, which could provide a more accurate model of TNR behavior within a three-way junction. Therefore, we performed chemical probing experiments on CAG sequences with an odd number of repeats.

Chemical Probe Analysis of Odd-Numbered, Single-Stranded TNR Sequences Lacking DNA Damage. When CAG7, CAG11, and CAG15 were incubated with DEPC, reactivity at every A in the sequence was observed, but hyper-reactivity was observed at adenines in the center of each sequence (Figure S3). Histograms displaying a graphical representation of the reactivity of each sequence are provided in Figure 3A and reveal that the adenines hyper-reactive toward DEPC are as follows: A3, A4, A5, and A7 in CAG7; A5, A6, and A7 in CAG11; and A7, A8, and A9 in CAG15. When each single-stranded substrate was incubated with DMS, reactivity was observed at each G, with hyper-reactivity observed at the guanines in the center and at the ends of each sequence: G1, G3, G4, and G7 in CAG7; G1, G5, and G6 in CAG11; and G1, G7, and G8 in CAG15 (Figure 3B and Figure S3).

The results obtained in the chemical probing experiments indicate the formation of stem−loop hairpins by CAG7, CAG11, and CAG15, with the most highly modified adenines and guanines in either the loop region or at the base of the stem (Figure 3C). The remaining adenines and guanines in the sequences participate in A·A mismatches and G−C base pairs in the stem. However, there are two scenarios which could produce the chemical reactivity profiles we observed for CAG7, CAG11, and CAG15, and both would be consistent with a stem−loop hairpin(s): (1) a homogeneous population of a single stem−loop with a 7 nucleobase loop and blunt-ended stem (Figure 3C(i)) or (2) a population consisting of two

dx.doi.org/10.1021/bi201552s | Biochemistry 2012, 51, 52−62

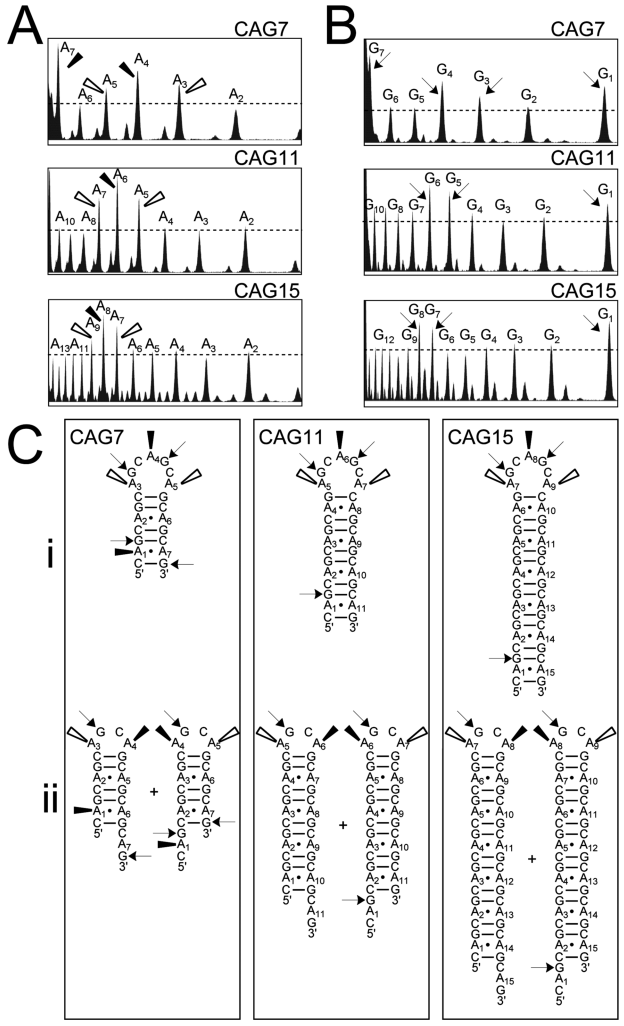

Figure 3. Histograms displaying reactivity of CAG7, CAG11, and CAG15 to (A) DEPC and (B) DMS. Histograms are derived from lanes 4 of the autoradiograms shown in Figure S3, in which the DNA was treated with the chemical probe at 37 °C for 15 min. The dashed line demarks the level of reactivity of adenines or guanines in the stem region, which serves as a baseline to establish hyper-reactivity of nucleobases in the loop. The closed wedge indicates the greatest degree of hyper-reactivity to DEPC, the open wedge indicates moderate hyper-reactivity to DEPC, and the arrow indicates hyper-reactivity to DMS. (C) Two potential scenarios for the structures of CAG7, CAG11, and CAG15 derived from their reactivity to DEPC and DMS. Structures containing a seven nucleobase loop and blunt-ended stem are shown in C(i) while a population of two stem–loops each containing a four nucleobase loop and either a 5′ or 3′ overhang is shown in C(ii).

different stem–loop structures, each with loops containing 4 nucleobases along with either a 5′ or 3′ overhang of one CAG repeat (Figure 3C(ii)).

Relative to the other guanines in the stem, the increased reactivity toward DMS observed at G1 in CAG7, CAG11, and CAG15 argues for the presence of a 5′ overhang, as G1 would be positioned in the stem in scenario (i) and would not be expected to have increased reactivity relative to G2. Since neither the stem–loop with the 5′ nor the 3′ overhang should be favored, we would expect both species to be present; therefore, in addition to the 5′ overhang indicated by hyper-reactivity to DMS at G1, we would also expect to observe a 3′ overhang. A 3′ overhang would be indicated by hyper-reactivity to DMS at G7, G11, and G15 for CAG7, CAG11, and CAG15, respectively. Indeed, hyper-reactivity at G7 of CAG7 was observed (Figure 3B), which is consistent with CAG7 forming a population of two stem–loop hairpins. However, because of the longer length of CAG11 and CAG15, we did not obtain sufficient electrophoretic resolution of the unmodified DNA from the fragment corresponding to cleavage induced by DMS at their respective 3′ guanines; this prevented direct observation of the 3′ overhang species for these substrates. Note that we used DMS, and not DEPC, to confirm the presence of overhangs in CAG7, CAG11, and CAG15; this is because an A1 fragment is not retained on the gel.

Structural Characterization of "Locked-Loop" Stem–Loop Standards. To confirm that CAG7, CAG11, and CAG15 form a population of two stem–loop structures as depicted in Figure 3C(ii), we mimicked both the blunt-ended and overhang stem–loop hairpins using "locked-loop" standards. We chose to derive the locked-loop standards from CAG7 as it possesses the same pattern of reactivity to chemical probes as the longer CAG11 and CAG15 substrates but also allows for electrophoretic resolution of unmodified DNA from DNA that is modified at the terminal 3′ repeat. In these standards, the nucleobases in the loop of the proposed CAG7 structure in either scenario (i) or (ii) are replaced by thymines, forcing the stem to adopt a 3′ overhang (CAG7-3′Overhang), a 5′ overhang (CAG7-5′Overhang), or a blunt-ended stem (CAG7-Blunt Stem) (Figure 4A,B). CAG7-3′Overhang and CAG7-5′Overhang

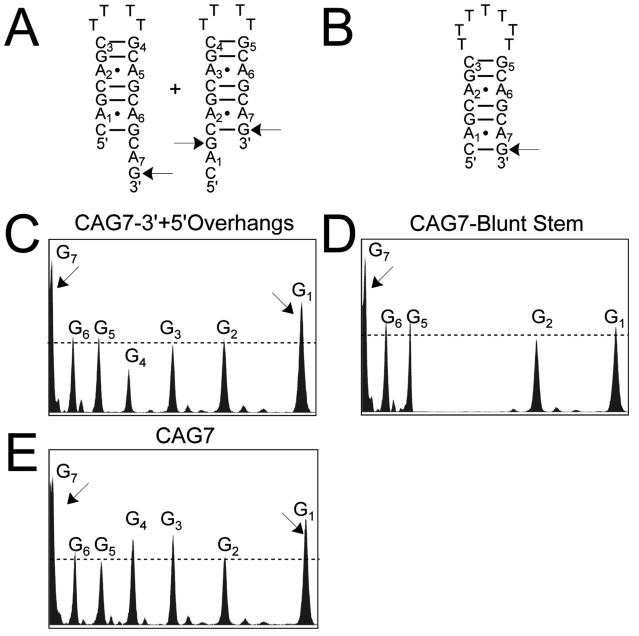

Figure 4. (A) Proposed structures for CAG7-3′Overhang (left) and CAG7-5′Overhang (right) and (B) CAG7-Blunt Stem. Histograms displaying reactivity to DMS for (C) CAG7-3′+5′Overhangs, (D) CAG7-Blunt Stem, and (E) and CAG7. Histograms are derived from lane 4 of the autoradiograms shown in Figures S4 and S5 where the DNA was treated with 0.05% (v/v) DMS at 37 °C for 15 min. The arrow indicates hyper-reactivity to DMS.

were combined in equal amounts to replicate the proposed population of structures with overhangs (CAG7-3′+5′Overhangs).

When incubated with DMS, both G1 and G7 of CAG7-3′+5′Overhangs display hyper-reactivity compared to the guanines in the neighboring repeats, consistent with the

dx.doi.org/10.1021/bi201552s | Biochemistry 2012, 51, 52–62

increased reactivity expected for the solvent-exposed overhangs (Figure 4C). Interestingly, while G7 of CAG7-Blunt Stem is hyper-reactive to DMS, G1 reacts at the same level as G2 (Figure 4D). For this blunt-ended substrate, the hyper-reactivity observed at G7 is likely due to end fraying of the stem, since this nucleobase is part of the terminal base pair. The reactions with DMS (Figure 4C and Figure S4) and DEPC (Figure S5) confirmed the expected folding of all locked-loop standards.

We then compared the reactivity of G1 and G7 toward DMS in the locked-loop CAG7 standards to the reactivity of the same nucleobases in CAG7. Since G1 and G7 of CAG7 display hyper-reactivity to DMS similar to that of the CAG7–3′+5′Overhangs standard (Figure 4E), and not that of CAG7-Blunt Stem, we conclude that CAG7 and the other odd-numbered repeat sequences, CAG11 and CAG15, form populations of two stem–loop hairpins with four nucleobase loops and either a 3′ or 5′ overhang (Figure 3C(ii)). Using enzymatic probes, other laboratories have proposed the presence of overhangs in structures formed by 15 CAG repeats.[29]

Influence of 8-OxoG on the Structure of an Odd-Numbered, Single-Stranded TNR DNA. The results discussed above demonstrate the adaptability of odd-numbered CAG repeats compared to CAG10. Thus, to better address the impact of 8-oxoG on the structure of TNR DNA and provide a better mimic for the stem–loop arm of the three-way junction, we performed chemical probe experiments with odd numbered substrates that contain 11 CAG repeats and in which a single G was site-specifically replaced by 8-oxoG. We chose CAG11 as the model substrate since it has the same number of base pairs and mismatches in the stem as CAG10 and the stem–loop arm of the three-way junction.

The first substrate contains 8-oxoG in the fifth repeat (CAG11-5OX), and the second substrate contains 8-oxoG in the sixth repeat (CAG11-6OX) (Table 1). As described above, upon incubation with DEPC, CAG11 that lacks DNA damage shows the highest degree of reactivity at A5, A6, and A7 (Figure 5B). The CAG11-5OX substrate has increased reactivity toward DEPC at A5 and A6 when compared to the flanking adenines (Figure 5C). This result indicates that A5 and A6 are part of the loop, while the remaining adenines are in A·A mismatches in the stem. In order for these particular adenines to be present in the loop, one CAG repeat must overhang at the 3′ end of the stem. In contrast to CAG11-5OX, in which A5 and A6 were most susceptible to modification by DEPC, CAG11-6OX displays increased reactivity at A6 and A7 (Figure 5D). This result indicates that CAG11-6OX also forms a stem–loop structure with a four nucleobase loop, but unlike CAG11-5OX, the loop includes A6 and A7. In this case one CAG repeat must overhang the 5′ end of the stem. As observed for CAG10, the two hyper-reactive adenines in CAG11-5OX and CAG11-6OX are modified by DEPC to different extents, which could be an effect of different stacking interactions with the adjacent bases. Notably, in both CAG11-5OX and CAG11-6OX the 8-oxoG is in the loop region.

We draw two conclusions from the chemical probing experiments of the CAG11 substrates. First, stem–loop TNR DNA containing 8-oxoG adopts a structure different from TNR DNA lacking the damage. The presence of the 8-oxoG imposes a structural constraint that results in formation of a *single* stem–loop, as compared to the CAG11 control that is a mixed population containing *two* species of stem–loop hairpins.

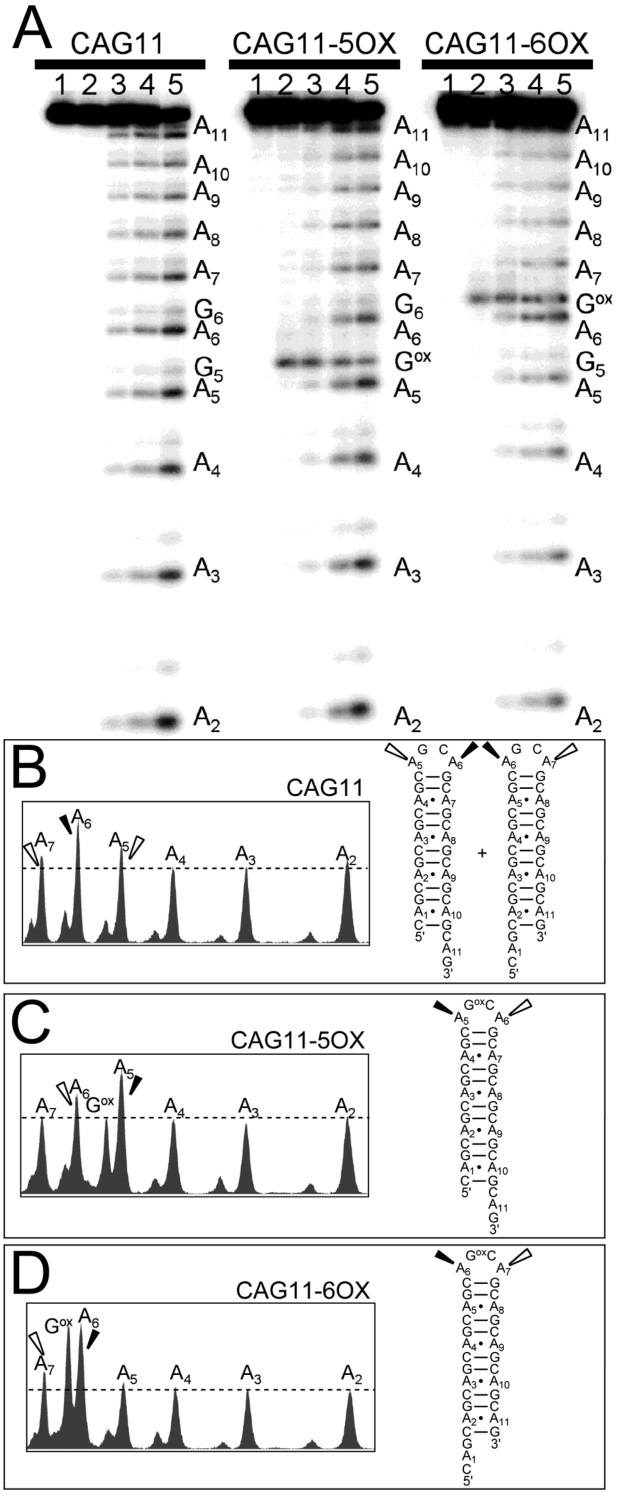

Figure 5. (A) Autoradiogram of DEPC reactions with CAG11, CAG11-5OX, and CAG11-6OX. Lanes 1 are DNA alone, lanes 2 are piperidine-treated DNA, and lanes 3–5 are DNA treated with 1% (v/v) DEPC at 37 °C for 5, 15, or 30 min, respectively, followed by treatment with piperidine. Histograms of DEPC reactivity, derived from lanes 4, with (B) CAG11, (C) CAG11-5OX, and (D) CAG11-6OX. The dashed line in each histogram demarks the level of reactivity of adenines in the stem region, which serves as a baseline to establish hyper-reactivity of the nucleobases in the loop. Proposed structures for CAG11, CAG11-5OX, and CAG11-6OX are shown next to the corresponding histogram. The closed wedge indicates the greatest degree of hyper-reactivity to DEPC and the open wedge indicates moderate hyper-reactivity to DEPC.

dx.doi.org/10.1021/bi201552s | *Biochemistry* 2012, 51, 52–62

Second, the position of the 8-oxoG within CAG11 determines the structure. Indeed, the stem–loop adapts in order to position 8-oxoG in the loop.

Calorimetric Analysis of Single-Stranded TNR DNA Lacking DNA Damage. To characterize further the structures adopted by the CAG7, CAG10, CAG11, and CAG15 sequences lacking 8-oxoG, we employed DSC to elucidate the thermal and thermodynamic parameters associated with the transition from the stem–loop hairpin to the unstructured state. Representative thermograms for CAG7, CAG10, CAG11, and CAG15 are shown in Figure 6. A DSC thermogram

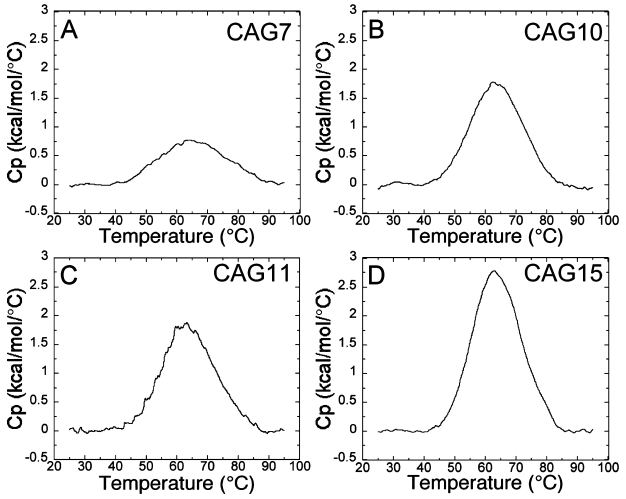

Figure 6. Representative thermograms, both background corrected using a buffer–buffer scan and baseline corrected using a polynomial fit, for (A) CAG7 at 33.1 μM, (B) CAG10 at 30 μM, (C) CAG11 at 16.8 μM, and (D) CAG15 at 40 μM. All samples were suspended in buffer containing 20 mM sodium phosphate, 70 mM NaCl, pH 7.5.

displays excess heat capacity as a function of temperature and the area under the curve is a direct measure of the enthalpy (ΔH) associated with the structural transition.[34] Entropy (ΔS), free energy (ΔG), and melting temperature (T_m) can be obtained as described previously.[34]

While there is an increase in the T_m between CAG7 and CAG10, and between CAG7 and CAG11, there is no significant difference in T_m between CAG10, CAG11, and CAG15 (Table 2). Previous work with CAG repeats, ranging in length from 6 to 25 repeats, has shown that, while there may be some fluctuations in T_m, the there is no linear relationship between T_m and repeat length.[29]

In contrast to the lack of linear relationship for T_m, we observed increasing ΔH values with respect to the length of the repeat sequence (Table 2), indicating that, as repeat length increases, so too does the enthalpic stability of the structure. With respect to nucleic acids, both hydrogen bonding and base stacking interactions are reflected in the value of ΔH.[34] Thus, the increase in ΔH observed here is rationalized by the increase in number of hydrogen bonds and base stacking interactions as the length of the stem increases. However, this increase in enthalpic stabilization as a function of TNR length is tempered by an increase in the entropic contributions. Nevertheless, ΔG increases with repeat length, indicating that the thermodynamic stability of the stem–loop hairpins increases with length. These thermodynamic data are consistent with previously reported, DSC-derived values for similarly sized CAG repeats that lack DNA damage.[22,29]

Analysis of Damage-Containing TNR Structures by Calorimetry. All of the 8-oxoG-containing sequences, composed of either 10 or 11 CAG repeats, show a decrease in T_m of ~2–4 °C compared to their undamaged control substrates, regardless of whether 8-oxoG is positioned in the loop or the loop-closing base pair (Table 2). It is known that 8-oxoG is thermally destabilizing when base-paired to C in a duplex,[17−19,35,36] although this is an example where 8-oxoG decreases T_m when present outside the context of a well-matched duplex. The decrease in T_m is likely caused by a modest perturbation of the base-stacking interactions in the loop when 8-oxoG is present, as supported by our chemical probing experiments.

With respect to the thermodynamic impact of 8-oxoG, we first considered its effects on the blunt-end CAG10 stem–loop hairpin. Compared to the undamaged CAG10 control, we observed no difference in the ΔH associated with the transition from the stem–loop to the unstructured sequence for CAG10-5OX, where 8-oxoG is positioned in the loop. When compared to the value for CAG10, there is a small but significant decrease in the ΔH for CAG10-6OX where the 8-oxoG is positioned in the loop-closing base pair (Table 2) (Figure S6). However, it is important to note that the $\Delta\Delta H$ of 4 kcal/mol observed for CAG10-6OX is much smaller than the values reported for 8-oxoG base-paired to C in a duplex, where $\Delta\Delta H$ values ranging from 7.3 to 52.9 kcal/mol have been reported depending on sequence context and length of the duplex.[17−19]

As observed for ΔH, ΔS is the same for CAG10 and CAG10-5OX, but there is a decrease in ΔS for CAG10-6OX compared to CAG10, indicating that the stem–loop formed by CAG10-6OX is more disordered than its counterparts. These changes in

Table 2. DSC-Derived Thermodynamic Parameters

substrate	T_m[a] (°C)	ΔH[a,b] (kcal/mol)	ΔS[a,b] (cal/(mol K))	ΔG[a,c] (kcal/mol)	$\Delta\Delta H$ (kcal/mol)	$\Delta\Delta S$ (cal/mol/K)	$\Delta\Delta G$ (kcal/mol)
CAG7	61.2 ± 1.3	23.7 ± 1.8	71.3 ± 5.2	1.72 ± 0.18			
CAG10	63.0 ± 0.5	33.8 ± 1.3	100.7 ± 4.0	2.63 ± 0.09	−10.1 ± 2.2[d]	−29.4 ± 6.6[d]	−0.9 ± 0.2[d]
CAG11	63.3 ± 0.1	34.0 ± 2.0	101.1 ± 6.0	2.67 ± 0.15	−10.3 ± 2.7[d]	−29.8 ± 7.9[d]	−1.0 ± 0.2[d]
CAG15	63.5 ± 0.7	51.4 ± 2.0	152.8 ± 6.1	4.00 ± 0.15	−27.7 ± 2.7[d]	−81.5 ± 8.1[d]	−2.3 ± 0.2[d]
CAG10-5OX	60.2 ± 0.7	33.4 ± 1.1	100.1 ± 3.2	2.34 ± 0.16	N/A[e,f]	N/A[e,f]	N/A[e,f]
CAG10-6OX	61.1 ± 0.5	29.8 ± 0.9	89.1 ± 2.5	2.15 ± 0.10	4.0 ± 1.8[e]	11.6 ± 4.7[e]	0.5 ± 0.1[e]
CAG11-5OX	59.5 ± 0.1	34.6 ± 2.7	104.1 ± 8.0	2.36 ± 0.18	N/A[e,f]	N/A[e,f]	N/A[e,f]
CAG11-6OX	59.5 ± 0.1	34.9 ± 2.6	104.9 ± 7.9	2.37 ± 0.19	N/A[e,f]	N/A[e,f]	N/A[e,f]

[a]DNA in 20 mM sodium phosphate, 70 mM NaCl, pH 7.5. The error represents the standard deviation derived from a minimum of three experiments. [b]Values derived by integration of the area under the excess heat capacity curve. [c]Values at 37 °C. [d]With respect to CAG7. [e]With respect to the equivalent substrate lacking 8-oxoG. [f]Not statistically different.

dx.doi.org/10.1021/bi201552s | Biochemistry 2012, 51, 52−62

ΔH and ΔS lead to a small but significant decrease in ΔG compared to CAG10, indicating that the structure formed by CAG10-6OX is thermodynamically less stable than the structures formed by either CAG10 or CAG10-5OX.

For CAG11 we observed that 8-oxoG does not influence ΔH. The $\Delta\Delta H$ comparing the melting transitions of CAG11-5OX and CAG11-6OX with the CAG11 control are nearly zero (Table 2) (Figure S6). The proposed structures for CAG11, CAG11-5OX, and CAG11-6OX have the same number of base pairs and mismatches in the stem and, therefore, the same number of hydrogen bonds (Figure 5). Thus, the hydrogen-bonding pattern is not expected to alter ΔH of the structures. 8-OxoG could potentially alter base stacking in the loop but given the similar ΔH values for the CAG11 substrates the contribution of base stacking to enthalpic stability must be similar for all substrates. Therefore, while our chemical probe data indicate that 8-oxoG alters base stacking in the loop, our thermodynamic data suggest that any alteration of stacking interactions caused by 8-oxoG in the loop of CAG11-5OX and CAG11-6OX is not sufficient to significantly alter the enthalpic stability of the stem–loop. Since it is known that 8-oxoG is enthalpically destabilizing when base paired with C in duplex,[17−19] 8-oxoG is likely positioned in the loop of these stem–loop structures to avoid the enthalpic penalty associated with base stacking and/or hydrogen bonding which would occur if 8-oxoG were in the stem region.

Here, we find that the positioning of 8-oxoG in the loop of TNR DNA decreases the T_m but does not affect ΔH. Another example where a modified nucleobase alters thermal, but not enthalpic, stability is 2-AP in a $(CAG)_6$ stem–loop hairpin.[37] When 2-AP was positioned in the loop, there was an increase in T_m, but there was no change in ΔH. Lee and co-workers proposed that the increase in thermal stability is a result of favorable base stacking interactions of 2-AP.

As observed for ΔH, the ΔS describing the transition from the structured to the unstructured state is the same for all three CAG11 substrates. It is reasonable to expect that the proposed structures would have similar degrees of disorder as each structure has the same number of G-C base pairs, A·A mismatches, and unpaired nucleobases. Thus, the similar ΔS values observed here indicate that 8-oxoG in the loop makes no significant contribution to the entropy of the system. Lastly, since 8-oxoG does not influence ΔH or ΔS of the stem–loop structure adopted by CAG11, the introduction of 8-oxoG to CAG11 does not affect the thermodynamic stability of the stem–loop hairpin.

Recent work done in the context of TNR Ω-DNA focused on investigating the thermodynamics of the tetrahydrofuran (THF) abasic site analogue, both alone and in combination with 8-oxoG, can broaden our understanding of the impact that 8-oxoG has on the structure of CAG repeat DNA.[38−40] The Ω-DNA is a three-way junction that contains an open bulge formed by 6 CAG repeats and is flanked on both sides by mixed-sequence duplex. On the basis of a calorimetric analysis, Völker and co-workers concluded that, because the Ω-DNA accommodates the THF abasic site without altering the thermodynamic parameters, the THF abasic site can alter the distribution of the structural microstates occupied by the Ω-DNA.[38] In other work, the same authors proposed allosteric coupling between a 8-oxoG and/or a THF abasic site in the Ω-DNA.[39,40] This finding again demonstrates the ability of these lesions to alter the microstates adopted by the Ω-DNA. Besides an abasic site, here we provide structural and thermodynamic data that support the notion that the CAG repeats can also adapt their structure to accommodate the oxidatively damaged nucleobase 8-oxoG.

Our results demonstrate that when 8-oxoG replaces G5 or G6 of CAG10, there is no overall change in the stem–loop structure. In contrast, when 8-oxoG replaces G5 or G6 of CAG11, the stem–loop structure changes to accommodate 8-oxoG in the loop, an adjustment that we propose is enthalpically driven. Why then does CAG10-6OX not position the 8-oxoG in the loop, and create a 5′ overhang, if a position in the loop is favored for 8-oxoG? If an overhang were to form, two base pairs in the stem would be lost, resulting in a decrease in $\Delta H \sim 10$ kcal/mol, using nearest-neighbor calculations.[41] The thermodynamic consequence arising from the loss of those base pairs would be more detrimental to the stability of the hairpin than the benefit that would come from positioning the 8-oxoG in the loop (+4 kcal/mol). Thus, the positioning of 8-oxoG in the TNR structure represents a thermodynamic balancing act; when there is the possibility of positioning 8-oxoG in the loop while still maintaining the base pairs and stacking of the stem, there is a significant favorability for 8-oxoG to occupy that position.

Reactions performed with DEPC showed the three-way junction CAG16-TWJ-8OX/CTG6-TWJ forms several unequivalent structures; the 8-oxoG occupies different positions within the stem–loop arm. Although DSC data obtained for the three-way junction could potentially yield thermodynamic parameters of the entire population, they cannot be used to determine the thermodynamic parameters of the individual structures. Importantly, we can use the thermodynamic information obtained for the CAG10 and CAG11 sequences to better understand the behavior of the stem–loop arm of the three-way junction. Because substitution of 8-oxoG at either G5 or G6 of CAG11 leads to formation of a single structure, we are able to determine thermodynamic parameters and evaluate the impact of the lesion on the TNR DNA by comparing to the unmodified substrate. In contrast to the enthalpic destabilization observed in duplex DNA, we have shown that 8-oxoG positioned in the loop of either a CAG10 or CAG11 stem–loop conveys no enthalpic penalty to the structure, and an 8-oxoG positioned in the loop closing base pair, as observed in CAG10-6OX, shows only a minor decrease in enthalpy, suggesting that positions in or near the loop are enthalpically favorable. It is of note that the structures lost upon addition of 8-oxoG to CAG16-TWJ/CTG6-TWJ are those that position the lesion furthest from the loop, where the lesion is expected to have the largest destabilizing effect.

■ CONCLUSIONS AND BIOLOGICAL IMPLICATIONS

Analysis via chemical probing revealed the ability of 8-oxoG to alter the population of structures formed by a three-way junction containing 16 CAG repeats. To better understand the innate ability of CAG repeat sequences to adapt to the presence of 8-oxoG, we performed the same chemical probe analysis on CAG10, which is identical in sequence to the stem–loop arm of the three-way junction as well as two CAG10 substrates containing 8-oxoG. We observed that 8-oxoG did not alter the structure of CAG10 and positioned 8-oxoG in either the loop or loop-closing base pair depending on the location of the lesion within the sequence. However, when 8-oxoG was introduced into CAG11, we observed a structural modification; 8-oxoG was positioned in the loop of both the CAG11-5OX and CAG11-6OX structures. The ability of the CAG11

dx.doi.org/10.1021/bi201552s | Biochemistry 2012, 51, 52−62

sequence to adapt its structure to accommodate the 8-oxoG lesion is likely due to the enthalpic penalty associated with the formation of an 8-oxoG-C base pair in the stem region.

The formation of stem–loop hairpins has been proposed to play a key role in mediating expansion by ligation of a structured flap into the repeat tract during LP-BER.[5−7,9,10] If 8-oxoG is present in the repeat tract as these structures form in the genome, they may form such that the 8-oxoG is positioned at or near the loop. Furthermore, if 8-oxoG forms within a stem–loop hairpin, the structure may rearrange to position the 8-oxoG in the loop. Importantly, our previous work has shown that 8-oxoG is inefficiently repaired when positioned in the loop of a stem–loop hairpin;[9] thus, 8-oxoG would persist and allow another round of the "toxic oxidation cycle" to occur. These results underscore the importance of understanding repeat structure and how the interplay with DNA damage can influence expansion of TNR regions in the genome.

■ ASSOCIATED CONTENT

Supporting Information

Histograms displaying reactivity of TWJ substrates with DEPC, reactivity of CAG10 substrates with DMS, reactivity of CAG7, CAG11, and CAG15 with DEPC and DMS, reactivity of locked-loop standards with DEPC and DMS, representative DSC thermograms for CAG10-5OX, CAG10-6OX, CAG11-5OX, CAG11-6OX, and supplementary discussion of piperidine-induced cleavage at 8-oxoG. This material is available free of charge via the Internet at http://pubs.acs.org.

■ AUTHOR INFORMATION

Corresponding Author

*Tel: (401) 863-3590. Fax: (401) 863-9368. E-mail: sarah_delaney@brown.edu.

Funding

This work was supported by the National Institute of Environmental Health Sciences (R01ES019296) and with Government support under and awarded by the Department of Defense, Air Force Office of Scientific Research, National Defense Science and Engineering Graduate (NDSEG) Fellowship, 32 CFR 168a, to C.B.V.

■ ACKNOWLEDGMENTS

We thank Craig Yennie and Amalia Ávila Figueroa for helpful discussions.

■ ABBREVIATIONS

ROS, reactive oxygen species; 8-oxoG, 8-oxo-7,8-dihydroguanine; Ogg1, 8-oxo-7,8-dihydroguanine glycosylase; TNR, trinucleotide repeat; HD, Huntington's disease; LP-BER, long-patch base excision repair; DEPC, diethyl pyrocarbonate; DMS, dimethyl sulfate; 2-AP, 2-aminopurine; DSC, differential scanning calorimetry.

■ REFERENCES

(1) Lindahl, T. (1993) Instability and decay of the primary structure of DNA. *Nature 362*, 709–715.

(2) Steenken, S., and Jovanovic, S. (1997) How Easily Oxidizable Is DNA? One-Electron Reduction Potentials of Adenosine and Guanosine Radicals in Aqueous Solution. *J. Am. Chem. Soc. 119*, 617–618.

(3) Burrows, C. J., and Muller, J. G. (1998) Oxidative Nucleobase Modifications Leading to Strand Scission. *Chem. Rev. 98*, 1109–1152.

(4) David, S. S., and Williams, S. D. (1998) Chemistry of Glycosylases and Endonucleases Involved in Base-Excision Repair. *Chem. Rev. 98*, 1221–1262.

(5) Kovtun, I. V., Liu, Y., Bjoras, M., Klungland, A., Wilson, S. H., and McMurray, C. T. (2007) OGG1 initiates age-dependent CAG trinucleotide expansion in somatic cells. *Nature 447*, 447–452.

(6) Liu, Y., Prasad, R., Beard, W. A., Hou, E. W., Horton, J. K., McMurray, C. T., and Wilson, S. H. (2009) Coordination between polymerase beta and FEN1 can modulate CAG repeat expansion. *J. Biol. Chem. 284*, 28352–28366.

(7) Goula, A.-V., Berquist, B. R., Wilson, D. M., Wheeler, V. C., Trottier, Y., and Merienne, K. (2009) Stoichiometry of base excision repair proteins correlates with increased somatic CAG instability in striatum over cerebellum In Huntington's disease transgenic mice. *PLoS Genet. 5*, e1000749.

(8) The Huntington's Disease Collaborative Research Group (1993) A novel gene containing a trinucleotide repeat that is expanded and unstable on Huntington's disease chromosomes. *Cell 72*, 971–983.

(9) Jarem, D. A., Wilson, N. R., and Delaney, S. (2009) Structure-dependent DNA damage and repair in a trinucleotide repeat sequence. *Biochemistry 48*, 6655–6663.

(10) Jarem, D. A., Wilson, N. R., Schermerhorn, K. M., and Delaney, S. (2011) Incidence and persistence of 8-oxo-7,8-dihydroguanine within a hairpin intermediate exacerbates a toxic oxidation cycle associated with trinucleotide repeat expansion. *DNA Repair 10*, 887–896.

(11) Ávila Figueroa, A., and Delaney, S. (2010) Mechanistic studies of hairpin to duplex conversion for trinucleotide repeat sequences. *J. Biol. Chem. 285*, 14648–14657.

(12) Ávila Figueroa, A., Cattie, D., and Delaney, S. (2011) Structure of even/odd trinucleotide repeat sequences modulates persistence of non-B conformations and conversion to duplex. *Biochemistry 50*, 4441–4450.

(13) Herr, W. (1985) Diethyl pyrocarbonate: a chemical probe for secondary structure in negatively supercoiled DNA. *Proc. Natl. Acad. Sci. U. S. A. 82*, 8009–8013.

(14) Degtyareva, N. N., Barber, C. A., Reddish, M. J., and Petty, J. T. (2011) Sequence length dictates repeated CAG folding in three-way junctions. *Biochemistry 50*, 458–465.

(15) Degtyareva, N. N., Reddish, M. J., Sengupta, B., and Petty, J. T. (2009) Structural studies of a trinucleotide repeat sequence using 2-aminopurine. *Biochemistry 48*, 2340–2346.

(16) Degtyareva, N. N., Barber, C. A., Sengupta, B., and Petty, J. T. (2010) Context dependence of trinucleotide repeat structures. *Biochemistry 49*, 3024–3030.

(17) Plum, G. E., Grollman, A. P., Johnson, F., and Breslauer, K. J. (1995) Influence of the oxidatively damaged adduct 8-oxode-oxyguanosine on the conformation, energetics, and thermodynamic stability of a DNA duplex. *Biochemistry 34*, 16148–16160.

(18) Chinyengetere, F., and Jamieson, E. R. (2008) Impact of the oxidized guanine lesion spiroiminodihydantoin on the conformation and thermodynamic stability of a 15-mer DNA duplex. *Biochemistry 47*, 2584–2591.

(19) Singh, S. K., Szulik, M. W., Ganguly, M., Khutsishvili, I., Stone, M. P., Marky, L. A., and Gold, B. (2011) Characterization of DNA with an 8-oxoguanine modification. *Nucleic Acids Res. 15*, 6789–6801.

(20) Maxam, A. M., and Gilbert, W. (1980) Sequencing end-labeled DNA with base-specific chemical cleavages. *Methods Enzymol. 65*, 499–560.

(21) Gacy, A. M., Goellner, G., Juranić, N., Macura, S., and McMurray, C. T. (1995) Trinucleotide repeats that expand in human disease form hairpin structures *in vitro*. *Cell 81*, 533–540.

(22) Paiva, A. M., and Sheardy, R. D. (2004) Influence of sequence context and length on the structure and stability of triplet repeat DNA oligomers. *Biochemistry 43*, 14218–14227.

(23) Paiva, A. M., and Sheardy, R. D. (2005) The influence of sequence context and length on the kinetics of DNA duplex formation from complementary hairpins possessing (CNG) repeats. *J. Am. Chem. Soc. 127*, 5581–5585.

(24) Pearson, C. E., and Sinden, R. R. (1996) Alternative structures in duplex DNA formed within the trinucleotide repeats of the myotonic dystrophy and fragile X loci. *Biochemistry 35*, 5041−5053.
(25) Pearson, C. E., Wang, Y. H., Griffith, J. D., and Sinden, R. R. (1998) Structural analysis of slipped-strand DNA (S-DNA) formed in $(CTG)_n$•$(CAG)_n$ repeats from the myotonic dystrophy locus. *Nucleic Acids Res. 26*, 816−823.
(26) Pearson, C. E., Tam, M., Wang, Y.-H., Montgomery, S. E., Dar, A. C., Cleary, J. D., and Nichol, K. (2002) Slipped-strand DNAs formed by long (CAG)*(CTG) repeats: slipped-out repeats and slip-out junctions. *Nucleic Acids Res. 30*, 4534−4547.
(27) Jarem, D. A., Huckaby, L. V., and Delaney, S. (2010) AGG interruptions in $(CGG)_{(n)}$ DNA repeat tracts modulate the structure and thermodynamics of non-B conformations in vitro. *Biochemistry 49*, 6826−6837.
(28) Amrane, S., and Mergny, J.-L. (2006) Length and pH-dependent energetics of (CCG)n and (CGG)n trinucleotide repeats. *Biochimie 88*, 1125−1134.
(29) Amrane, S., Saccà, B., Mills, M., Chauhan, M., Klump, H. H., and Mergny, J.-L. (2005) Length-dependent energetics of $(CTG)_n$ and $(CAG)_n$ trinucleotide repeats. *Nucleic Acids Res. 33*, 4065−4077.
(30) Zheng, M., Huang, X., Smith, G. K., Yang, X., and Gao, X. (1996) Genetically unstable CXG repeats are structurally dynamic and have a high propensity for folding. An NMR and UV spectroscopic study. *J. Mol. Biol. 264*, 323−336.
(31) Mitas, M. (1997) Trinucleotide repeats associated with human disease. *Nucleic Acids Res. 25*, 2245−2254.
(32) Huertas, D., Bellsolell, L., Casasnovas, J. M., Coll, M., and Azorín, F. (1993) Alternating $d(GA)_n$ DNA sequences form antiparallel stranded homoduplexes stabilized by the formation of G•A base pairs. *EMBO J. 12*, 4029−4038.
(33) Bhattacharya, P. K., Cha, J., and Barton, J. K. (2002) ^{1}H NMR determination of base-pair lifetimes in oligonucleotides containing single base mismatches. *Nucleic Acids Res. 30*, 4740−4750.
(34) Marky, L. A., and Breslauer, K. J. (1987) Calculating thermodynamic data for transition of any molecularity from equilibrium melting curves. *Biopolymers 26*, 1601−1620.
(35) McAuley-Hecht, K. E., Leonard, G. A., Gibson, N. J., Thomson, J. B., Watson, W. P., Hunter, W. N., and Brown, T. (1994) Crystal structure of a DNA duplex containing 8-hydroxydeoxyguanine-adenine base pairs. *Biochemistry 33*, 10266−10270.
(36) Oda, Y., Uesugi, S., Ikehara, M., Nishimura, S., Kawase, Y., Ishikawa, H., Inoue, H., and Ohtsuka, E. (1991) NMR studies of a DNA containing 8-hydroxydeoxyguanosine. *Nucleic Acids Res. 19*, 1407−1412.
(37) Lee, B. J., Barch, M., Castner, E. W., Völker, J., and Breslauer, K. J. (2007) Structure and dynamics in DNA looped domains: CAG triplet repeat sequence dynamics probed by 2-aminopurine fluorescence. *Biochemistry 46*, 10756−10766.
(38) Völker, J., Plum, G. E., Klump, H. H., and Breslauer, K. J. (2009) DNA repair and DNA triplet repeat expansion: the impact of abasic lesions on triplet repeat DNA energetics. *J. Am. Chem. Soc. 131*, 9354−9360.
(39) Völker, J., Plum, G. E., Klump, H. H., and Breslauer, K. J. (2010) Energetic coupling between clustered lesions modulated by intervening triplet repeat bulge loops: allosteric implications for DNA repair and triplet repeat expansion. *Biopolymers 93*, 355−369.
(40) Völker, J., Plum, G. E., Klump, H. H., and Breslauer, K. J. (2010) Energy crosstalk between DNA lesions: Implications for allosteric coupling of DNA repair and triplet repeat expansion pathways. *J. Am. Chem. Soc. 132*, 4095−4097.
(41) SantaLucia, J. (1998) A unified view of polymer, dumbbell, and oligonucleotide DNA nearest-neighbor thermodynamics. *Proc. Natl. Acad. Sci. U. S. A. 95*, 1460−1465.